MODELS FOR THE COMBUSTION OF INDIVIDUAL PARTICLES OF VARIOUS COAL TYPES

Chun Wei Lau and Stephen Niksa*
High Temperature Gasdynamics Laboratory
Stanford University, Stanford, CA 94305

Keywords: Modeling, coal combustion, soot, coal type effects

INTRODUCTION

Our modeling aims to identify the chemical processes and transport mechanisms underlying differences in the ways that different types of coal burn. At this point, thermal histories and audits of the heat release from individual particles are emphasized. Three limiting cases have been formulated for this comparative study. In one scenario, the noncondensible gases and tars from primary devolatilization are consumed by combustion in envelope diffusion flames around individual particles. The devolatilization products from different coals are distinguished by different evolution rates, elemental compositions, average molecular weights, and transport properties. In another modeling scenario, the products of primary devolatilization are radically transformed by secondary pyrolysis after they are expelled from the coal until only H_2, CO, C_2H_2, CO_2, H_2O, and soot remain. This scenario also develops separate limiting behavior for instantaneous soot oxidation in envelope flames and for frozen soot oxidation chemistry. Thermophoresis and radiation are accounted for in this transport analysis. Comparisons among predicted and observed flame lifetimes and maximum flame standoffs indicate that transport-limited oxidation of secondary pyrolysis products, including soot, is the most realistic modeling scenario.

DESCRIPTION OF THE MODELS

Formal developments of all 3 models are available (1,2). The model that describes tar and gas combustion is denoted by FSCM-FSP for "Flame Sheet Coal Combustion Model with Frozen Secondary Pyrolysis." The two models with soot instead of tar are denoted by FSCM-ISP/ISO and FSCM-ISP/FSO where "ISP" denotes infinitely-fast secondary pyrolysis, and the modifiers "ISO" and "FSO" denote infinitely-fast and frozen soot oxidation, respectively. All scenarios account for primary devolatilization (with FLASH2 (3)), multicomponent diffusion and Stefan flow, fuel accumulation between the particle surface and flame sheet, instantaneous volatiles combustion, and heterogeneous oxidation of char into CO. The common heat transfer mechanisms are the fuel particle's thermal capacitance and radiation flux, heat conduction from the particle and flame, advection of sensible enthalpy, and the heats of pyrolysis, char oxidation, and volatiles combustion. Flame temperatures and the distribution of combustion products are based on thermochemical equilibrium among 12 species, including dissociation fragments.

Both of the FSCM-ISP models invoke infinitely-fast conversion of tar into soot, so only soot and noncondensibles are ejected from the particle into the gas film. The elements in tar are apportioned into soot having a C/H ratio of 9, the ultimate value for any coal type, and appropriate amounts of H_2 and CO. Noncondensibles compositions are adjusted further to eliminate the amount of C_2H_2 that maintains equal masses of soot and tar, consistent with recent laboratory studies. Soot's Brownian diffusivity is considerably lower that tars', and the inverted temperature profile from particle to flame drives thermophoresis that counteracts its Brownian and convective transport.

*Current address: Molecular Physics Laboratory, SRI International
333 Ravenswood Avenue, Menlo Park, CA 94025

RESULTS

As fuels, soot and noncondensible gases from different coals have the characteristics in Table 1. Total weight loss tends to be the same for all ranks through hv bituminous then falls off for medium and low volatile bituminous coals, and vanishes for anthracites. Yields of noncondensibles decrease monotonically with rank, so soot yields are maximized with hv bituminous samples. The stoichiometric ratios and lower heating values of soot from the four coal types mimic the trends in tar characteristics, but values for soot are higher. The stoichiometry for gas combustion increases with rank, reflecting less dilution by CO_2, H_2O, and other oxygenated species.

Temperature histories and flame trajectories from all 3 models appear in Fig. 1. These simulations are for 70 μm Pit. #8 particles injected into a stream of 8% O_2 in N_2 at 1500 K within a conduit at 900 K. When sooting is ignored, flame temperatures (Fig. 1a) reach the hottest maximum value (2600 K) because tar/gas flames penetrate furthest into the film (Fig. 1b). Soot/gas flames are much cooler, reaching only 2320 K, and stay closer to their particles. Note, however, the particle heating rate from FSCM-ISP/ISO is substantially higher than from FSCM-FSP, by virtue of radiation from soot to the particle. Flames from FSCM-ISP/ISO last longer than from FSCM-FSP, even though the particle heating rates from FSCM-ISP/ISO are faster. Clearly, radiation from soot to the particle is also significant, accounting for up to one-third of the conduction flux to the particle at the point of maximum flame standoff. On a cumulative basis, 12% of the heat of volatiles combustion is radiated back to the particle..

Calculations from FSCM-ISP/FSO which omit soot oxidation predict much cooler temperature histories for flames and particles (Fig. 1a). Because of their low oxygen requirements, gas flames sit close to the particle, penetrating only up to 4 radii into the film, and have the shortest pathway for conductive feedback. Also, the extent of the soot layer increases without bound when soot survives the flame, so radia-tion losses also grow continuously. Consequently, the flame temperature from FSCM-ISP/FSO reaches the implausibly low value of 1800 K.

With the FSCM-ISP models, macroscopic features of the Pit. #8 are fairly representative of the other coal types. Maximum flame temperatures in Table 2 vary by less than 200 K. Qualitatively, the same rank-dependence is seen with FSCM-FSP. But quantitatively, sooting suppresses the rank dependence because soot radiation is strongest for coals with the largest soot yields. Soot radiation cools flames on Pit. #8 particles by 300 K, but for Zap and Poc. coals the reduction is only 200 K, so differences are reduced. Flame radii also become more insensitive to coal rank when sooting is included.

Because of their similar flame temperatures, audits of the energy release based on FSCM-ISP/ISO are also similar for all coal types. For 100 μm particles, roughly one-third is transferred into the surroundings while 60% is radiated or conducted back to the particle. Only a few percent is carried away by intermediate species. Since flame standoffs depend on particle size, the fractional energy feedback to the particle is also size-dependent. For sizes larger than the threshold for attached flames, the fraction fedback increases for smaller sizes, exceeding 90% at the critical size for all coal types. The critical sizes for heterogeneous combustion indicate the size at which oxygen transport is fast enough to consume all volatiles and oxidize the char on the particle surface, in an "attached" flame. These values are virtually identical for all 3 models.

Only flame durations and maximum standoffs monitored in a drop tube furnace (4) are available to evaluate the different modeling scenarios. Actual particle sizes, coal properties, gas temperatures, and O_2 levels are used in the simulations, but none of the modeling parameters were adjusted or specified to improve the fit of the model predictions. Observed flame durations are plotted with predictions for Ill. #6 coal in Fig. 2a. Predictions from FSCM-FSP and FSCM-ISP/ISO are within experimental uncertainty, but those from FSCM-ISP/FSO are too long at all O_2 levels. The evaluation of flame standoffs for the same coal appears in Fig. 2b. Here differences among the 3 models are somewhat more discriminating. Predicted standoffs from SFCM-ISP/ISO provide the closest match, although FSCM-FSP/FSO predictions are also within experimental uncertainty. But FSCM-ISP/FSO predictions are much too low.

DISCUSSION

These simulations are the basis for several recommendations regarding models to predict the macroscopic combustion characteristics of the initial stages of pulverized coal combustion. Flame durations are governed by the evolution of primary devolatilization products, not heat or mass transport, and flame trajectories and maximum standoffs are primarily governed by the stoichiometric oxygen requirements of the fuel and fuel species accumulation. So these aspects are insensitive to soot formation. Likewise, the ways that particle sizes and the oxygen levels and temperatures in the free stream affect combustion characteristics are also insensitive to sooting. In contrast, reliable flame temperatures and concentration and temperature profiles can only be computed from models that account for the radiation heat transfer and thermophoretic mass transfer of soot. Although we have not yet expanded this model to represent NO_x formation, it is worth noting that the fuel species concentration profiles between particle surfaces and flame sheets are also significantly affected by thermophoretic and Brownian transport of soot. Both of these mechanisms enhance the accumulation of soot in the film, thereby flattening the fuel concentration profiles throughout.

REFERENCES

1. Lau, C.-W., and Niksa, S., Combust. Flame, 1992, **90**, 45.

2. Lau, C.-W., and Niksa, S., Combust. Flame, 1993, to appear.

3. Niksa, S., AIChE J., 1988, 43, 790.

4. Timothy, L. D., Froelich, D., Sarofim, A. E., Beer, J. M., Twenty-First Int. Symp. on Combust., 1986, 1141, The Combustion Institute, Pittsburgh, PA.

Table 1. Combustion Characteristics of Secondary Pyrolysis Products From Four Coals.

	Zap	Ill. #6	Pit. #8	Poc.
Ultimate Yield, wt. %daf				
Soot	20.4	26.7	35.7	15.5
Gases	33.3	25.3	19.0	8.3
Molar Stoichiometry				
Soot Combustion	36.5	31.6	27.9	25.6
Gas Combustion	0.33	0.80	0.83	1.10
$\Delta H_C°$, kJ/mole				
Soot	1.5×10^4	1.4×10^4	1.3×10^4	1.2×10^4
Gases	3.4×10^2	4.9×10^2	5.0×10^2	5.6×10^2
All Volatiles	4.4×10^2	1.3×10^3	1.8×10^3	1.4×10^3

Table 2. Selected Combustion Characteristics For the Four Coals From FSCM-ISP/ISO.

	Zap	Ill. #6	Pit. #8	Poc.
Max. Flame Temp., K	2130	2190	2320	2160
Max. Flame Standoff, particle radii	5.4	6.0	7.0	5.8
Critical Sizes for Hetero. Combustion Mode, µm	18.2	15.8	8.0	27.8
Energy Fraction Fedback to Particle	0.61	0.62	0.56	0.64
Energy Fraction Lost to Free Stream	0.33	0.32	0.32	0.30

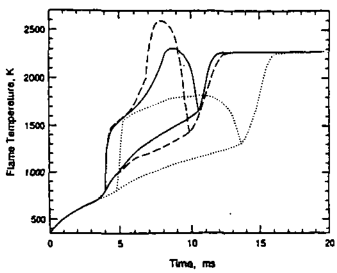

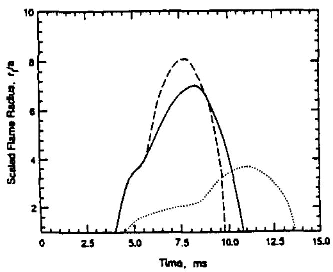

Fig. 1 (a) Transient particle and flame temperatures for base operating conditions based on FSCM-FSP (dashed curve) FSCM-ISP/ISO (solid curve) and FSCM-ISP/FSO (dotted curve).

Fig. 1 (b) Flame trajectories based on FSCM-FSP (dashed curve), FSCM-ISP/ISO (solid curve), and FSCM-ISP/FSO.

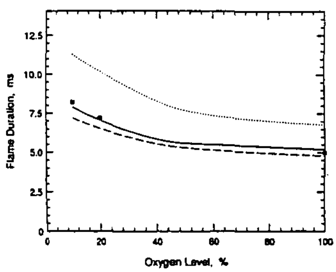

(a)

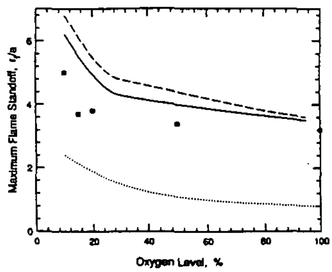

(b)

Fig. 2(a). Predicted flame durations for the Ill. #6 coal based on FSCM-FSP (dashed curve), FSCM-ISP/ISO (solid curve), and FSCM-ISP/FSO (dotted curve) compared to measured values [4] for a Utah hv bituminous coal of similar composition. At all oxygen levels, the size is 100 μm and the gas temperature is 1250 K.

Fig. 2(b). Predicted maximum flame standoffs for the Ill. #6 coal based on FSCM-FSP (dashed curve), FSCM-ISP/ISO (solid curve), and FSCM-ISP/FSO (dotted curve) compared to measured values [4] for a Utah hv bituminous coal of similar composition. At all oxygen levels, the size is 100 μm and the gas temperature is 1250 K.